

# Ligand-directed targeting of lymphatic vessels uncovers mechanistic insights in melanoma metastasis

Dawn R. Christianson<sup>a,1,2</sup>, Andrey S. Dobroff<sup>b,c,1</sup>, Bettina Proneth<sup>a,1,3</sup>, Amado J. Zurita<sup>d</sup>, Ahmad Salameh<sup>a,4</sup>, Eleonora Dondossola<sup>a</sup>, Jun Makino<sup>e</sup>, Cristian G. Bologa<sup>f</sup>, Tracey L. Smith<sup>b,c</sup>, Virginia J. Yao<sup>b,c</sup>, Tiffany L. Calderone<sup>g</sup>, David J. O'Connell<sup>h</sup>, Tudor I. Oprea<sup>f</sup>, Kazunori Kataoka<sup>i</sup>, Dolores J. Cahill<sup>h</sup>, Jeffrey E. Gershenwald<sup>g</sup>, Richard L. Sidman<sup>i,5</sup>, Wadih Arap<sup>b,k,5</sup>, and Renata Pasqualini<sup>b,c,5</sup>

<sup>a</sup>David H. Koch Center and Departments of <sup>d</sup>Genitourinary Medical Oncology and <sup>g</sup>Surgical Oncology, The University of Texas MD Anderson Cancer Center, Houston, TX 77030; <sup>b</sup>University of New Mexico Cancer Center and Divisions of <sup>c</sup>Molecular Medicine, <sup>f</sup>Translational Informatics, and <sup>k</sup>Hematology and Medical Oncology, Department of Internal Medicine, University of New Mexico School of Medicine, Albuquerque, NM 87131; <sup>e</sup>Center for Disease Biology and Integrative Medicine, Graduate School of Medicine, and <sup>h</sup>Department of Bioengineering, Graduate School of Engineering, University of Tokyo, Tokyo 113-0033, Japan; <sup>i</sup>Conway Institute of Biomedical and Biomolecular Science, University College Dublin, Belfield, Dublin 4, Ireland; and <sup>1</sup>Department of Neurology, Beth Israel Deaconess Medical Center, Harvard Medical School, Boston, MA 02215

Contributed by Richard L. Sidman, January 9, 2015 (sent for review December 5, 2014)

**Metastasis is the most lethal step of cancer progression in patients with invasive melanoma. In most human cancers, including melanoma, tumor dissemination through the lymphatic vasculature provides a major route for tumor metastasis. Unfortunately, molecular mechanisms that facilitate interactions between melanoma cells and lymphatic vessels are unknown. Here, we developed an unbiased approach based on molecular mimicry to identify specific receptors that mediate lymphatic endothelial-melanoma cell interactions and metastasis. By screening combinatorial peptide libraries directly on afferent lymphatic vessels resected from melanoma patients during sentinel lymphatic mapping and lymph node biopsies, we identified a significant cohort of melanoma and lymphatic surface binding peptide sequences. The screening approach was designed so that lymphatic endothelium binding peptides mimic cell surface proteins on tumor cells. Therefore, relevant metastasis and lymphatic markers were biochemically identified, and a comprehensive molecular profile of the lymphatic endothelium during melanoma metastasis was generated. Our results identified expression of the phosphatase 2 regulatory subunit A,  $\alpha$ -isoform (PPP2R1A) on the cell surfaces of both melanoma cells and lymphatic endothelial cells. Validation experiments showed that PPP2R1A is expressed on the cell surfaces of both melanoma and lymphatic endothelial cells in vitro as well as independent melanoma patient samples. More importantly, PPP2R1A-PPP2R1A homodimers occur at the cellular level to mediate cell-cell interactions at the lymphatic-tumor interface. Our results revealed that PPP2R1A is a new biomarker for melanoma metastasis and show, for the first time to our knowledge, an active interaction between the lymphatic vasculature and melanoma cells during tumor progression.**

cell-cell interaction | cell surface peptide | lymphatic targeting | phage display

Despite the similarities between the lymphatic and blood vasculature, lymphatic vessels (LyVs) have their own distinct morphological and molecular profile (1, 2). The lymphatic vasculature plays a critical role in the pathogenesis of many diseases, including inflammatory disorders, lymphedema, tumor progression, and metastasis. The role of LyVs in tumor dissemination and metastasis has been recognized and correlates with the number of tumor-associated LyVs with lymph node (LN) metastasis (3–5). In fact, the degree of LN involvement has become a good prognostic indicator of patient outcome in several human tumors, including melanoma (6). Surgical resection of the primary tumor and regional LN is the best treatment option for early-stage disease. However, early detection of in-transit melanoma or successful identification of metastasis-positive LN remains a major challenge for clinicians because of the lack of reliable LN markers and sensitive detection techniques.

As the malignant phenotype of melanoma cells transitions from the noninvasive radial growth phase to the vertical growth phase (metastatic phenotype), the repertoire of proteins expressed on the cell surface, such as adhesion molecules and matrix-degrading enzymes, does as well (7–9). These molecular changes enable complex interactions of metastatic cells with the extracellular milieu to propel the spread of disease. Moreover, growing evidence implicates that soluble tumor factors, such as VEGF-C and VEGF-D, induce lymphangiogenesis in LNs before the arrival of tumor cells, thus creating a so-called “premetastatic niche” (10–13). However, the mechanisms by which tumor cells leave the primary tumor, invade the lymphatic system, and spread to regional LN and distant organs are highly complex and may involve additional yet to be identified molecules that facilitate cell-cell attraction, adhesion, and migration. Here, we developed a rapid ex vivo screening technology based on molecular mimicry to identify novel cell-cell interacting ligands involved in the interplay between tumor cells and lymphatic endothelial cells (LECs) that potentially promote metastasis.

## Significance

**Formation of metastasis is the most deadly step in melanoma progression and primarily occurs through the lymphatic vasculature. Unfortunately, little is known regarding the underlying molecular mechanisms that enable interactions between melanoma cells and lymphatic vessels. In this study, we developed an unbiased approach using combinatorial peptide libraries displayed on phage coat proteins to identify cell-cell interacting proteins at the lymphatic vessel-tumor cell interface. Successful application of this approach led to the identification of cell surface PPP2R1A on both melanoma and lymphatic cell surfaces, and more importantly, PPP2R1A facilitates tumor cell-lymphatic endothelial cell interactions during melanoma cell metastasis.**

Author contributions: D.R.C., A.S.D., B.P., A.J.Z., E.D., D.J.C., J.E.G., R.L.S., W.A., and R.P. designed research; D.R.C., A.S.D., B.P., A.J.Z., A.S., E.D., J.M., T.L.C., and D.J.O. performed research; D.R.C., A.S.D., B.P., A.J.Z., E.D., J.M., C.G.B., and T.I.O. analyzed data; and D.R.C., A.S.D., B.P., E.D., T.L.S., V.J.Y., K.K., J.E.G., R.L.S., W.A., and R.P. wrote the paper.

The authors declare no conflict of interest.

Freely available online through the PNAS open access option.

<sup>1</sup>D.R.C., A.S.D., and B.P. contributed equally to this work.

<sup>2</sup>Present address: Arrowhead Research Corporation, Pasadena, CA 91101.

<sup>3</sup>Present address: Helmholtz Zentrum München, Neuherberg 85764, Germany.

<sup>4</sup>Present address: Brown Foundation Institute of Molecular Medicine, University of Texas Health Science Center at Houston, Houston, TX 77030.

<sup>5</sup>To whom correspondence may be addressed. Email: richard\_sidman@hms.harvard.edu, warap@salud.unm.edu, or rpassqual@salud.unm.edu.

This article contains supporting information online at [www.pnas.org/lookup/suppl/doi:10.1073/pnas.1424994112/-DCSupplemental](http://www.pnas.org/lookup/suppl/doi:10.1073/pnas.1424994112/-DCSupplemental).

Phage display has been successfully exploited *in vitro*, *ex vivo*, and *in vivo* to decipher the molecular diversity of peptide binding specificity to isolated proteins, purified antibodies (Abs), cell surface receptors, and intracellular/cytoplasmic domains (14–17). The novelty of our lymphatic screen was the availability of intact human afferent LyVs obtained from melanoma patients during intraoperative lymphatic mapping and sentinel LN biopsies (18, 19). Additional studies on selected peptides allowed us to biochemically identify several relevant metastasis and lymphatic markers to generate a comprehensive molecular profile of the lymphatic endothelium during melanoma metastasis. We identified cell surface expression of phosphatase 2 regulatory subunit A,  $\alpha$ -isoform (PPP2R1A) (20) on both melanoma cells and LECs. Furthermore, *in vitro* studies revealed that PPP2R1A mediates a heterotypic cell–cell interaction through homodimer formation. Finally, PPP2R1A is expressed at high levels in melanoma patient samples, thus highlighting its functional role during melanoma progression and metastasis.

## Results

**Mapping the Lymphatic Endothelium in Melanoma.** To map specific proteins that participate in LEC–melanoma cell interactions, we developed a unique two-arm screening method based on phage display (step 1) (Fig. 1A) and the “molecular mimicry” approach (step 2) (Fig. 1B). In step 1, segments of afferent LyVs were isolated from residual tissues of sentinel LN biopsy procedures from melanoma patients. A combinatorial peptide library displayed on phage, comprising seven random amino acid peptides constrained by two cysteines (CX<sub>7</sub>C), was screened directly in the lumen of isolated LyV. In each consecutive round, the enriched phage pool from the previous round was used as the input. In round 1, LyV segments of six patients were used to account for interpatient variability and ensure an adequately diverse phage pool for round 2 on LyV and primary LECs. For rounds 2 and 3, LyV segments from four different patients were used ( $n = 14$  patient-derived LyVs). In parallel, the peptides enriched from round 1 from the LyV screening were subjected to three additional rounds of screening with early-passage LECs. LEC screenings (rounds 2–4) were carried out with the Biopanning and Rapid Analysis of Selective Interactive Ligands approach (21, 22). Phages recovered from each round, except round 1, were sequenced, and peptide abundance was determined. Four peptides (GLTFKSL, VSQRNEL, FSGWSTV, and AEKSSYV) were enriched (Fig. 1C). These enriched sequences were also present in the phage pool recovered after round 3 of the LyV screening, indicating that the identified peptides bind to a receptor accessible from the luminal side.

Next (step 2), rabbits were immunized against the four enriched peptides, and polyclonal Abs were affinity-purified. To test if the anti-peptide sera recognized cell surface proteins on melanoma cells, immunofluorescence experiments were performed with the sera as a primary Ab pool. Anti-GLTFKSL Abs bound strongly to a protein expressed on the cell surface in a high percentage of C8161 melanoma cells (Fig. 1D), and very little binding was found with the AEKSSYV, FSGWSTV, or VSQRNEL Abs. C8161 cells were not immunoreactive against the preimmune control serum. Based on these results, we decided to pursue further studies with the GLTFKSL ligand/receptor pair. To validate additionally that the GLTFKSL peptide mimics a relevant membrane protein, we performed a phage-based binding assay with LECs derived from melanoma patients, human umbilical vein endothelial cells, and C8161 melanoma cells. Phage displaying the GLTFKSL peptide preferentially bound to LECs as well as C8161 cells compared with human umbilical vein endothelial cells, whereas an insertless control phage (Fd phage) did not bind any of the cell types (Fig. 1E). Immunofluorescence studies were performed on human dermal LECs (HDLECs) or LECs with intact membranes (nonpermeabilized) and permeabilized cells to

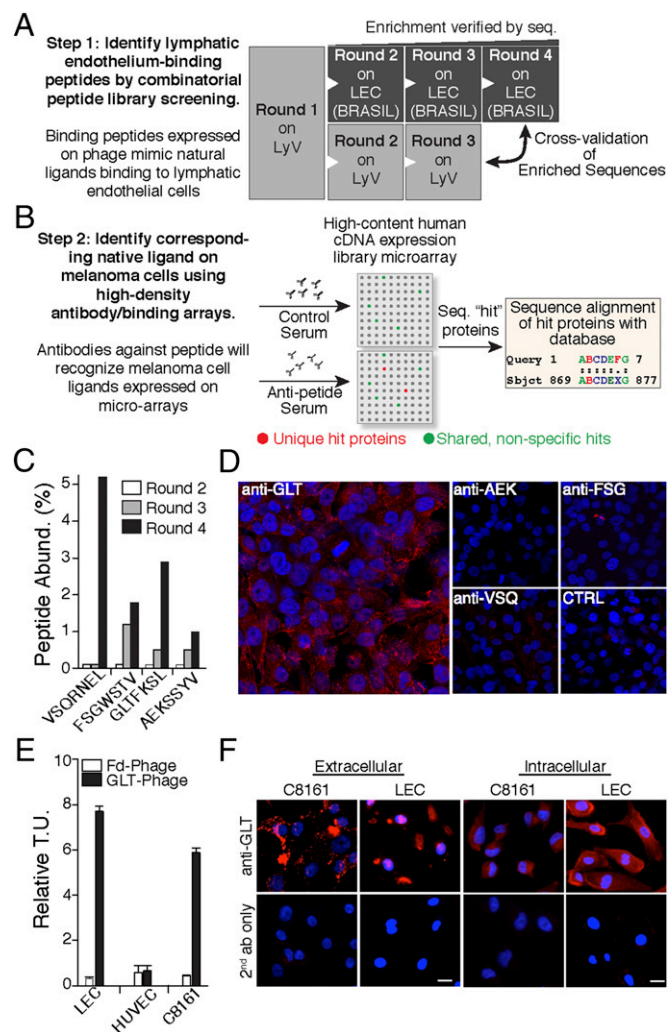


**Fig. 1.** Two-step screening methodology based on molecular mimicry. (A) Flowchart depicting the separate screenings based on an LyV culture and consecutive LEC screening rounds with the Biopanning and Rapid Analysis of Selective Interactive Ligands (BRASIL) method. (B) Identification of the native protein-mimicking ligands with high-density protein microarrays. Anti-peptide serum and control serum reactivity to proteins on a nitrocellulose-dotted human microarray was evaluated. (C) Sequences of peptides enriched during rounds 2–4. The enrichment was calculated based on peptide abundance from the total number of peptides sequenced. (D) Melanoma cell immunoreactivity against the corresponding anti-peptide sera by immunofluorescence. Anti-GLTFKSL serum recognizes a protein on the cell surface of C8161 melanoma cells compared with anti-AEKSSYV, anti-FSGWSTV, anti-VSQRNEL, and negative control serum. (E) Specific peptide cell surface binding to LECs and C8161 melanoma cells. Binding of GLTFKSL displayed on phage was evaluated using the BRASIL method. GLTFKSL phage specifically bound to LECs and C8161 melanoma cells compared with insertless control phage (Fd phage) and human umbilical vein endothelial cells (HUVECs). Relative transducing units (T.U.) are displayed as means  $\pm$  SEMs. (F) Nonpermeabilized and permeabilized LECs and melanoma cells were immunoreactive against GLTFKSL Abs.

confirm the specificity of the anti-GLTFKSL Ab to both lymphatic and melanoma cells (Fig. 1F). In permeabilized cells, the GLTFKSL Ab specifically stained the intracellular compartment. In contrast, when cells with intact membranes were used, a distinct cell surface immunostaining was observed for both LECs and melanoma cells. Collectively, these results indicated that the GLTFKSL ligand/receptor pair is involved in lymphatic endothelium–melanoma cell interactions.

To identify the endogenous protein that the GLTFKSL peptide mimics, anti-GLTFKSL serum was exposed to a human

recombinant protein array consisting of 37,200 redundant proteins from a human fetal brain cDNA expression library. Each protein is expressed in duplicate in a grid-like pattern, and a positive hit is considered unique when a protein is detected in duplicate on the array incubated with antipeptide serum and not detected in the array incubated with control serum. The GLTFKSL immune serum specifically recognized two distinct proteins, which were sequenced and subjected to protein database searching with BLAST. Two unique positive protein hits were identified and derived from the same protein–protein PPP2R1A. The sequence of these two clones had a 100% identity match to the PPP2R1A protein, with one clone spanning residues 474–589 and the other one corresponding to residues 457–589 (Fig. S1).

**Validation of PPP2R1A Membrane Expression.** To verify that the GLTFKSL Ab recognizes PPP2R1A, the residues 457–589 from PPP2R1A were expressed and purified. As expected, the purified PPP2R1A fragment was recognized by the GLTFKSL Ab by Western blot analysis, whereas a control protein was not immunoreactive (Fig. 2A). Additionally, binding of GLTFKSL Abs to the recombinant PPP2R1A fragment was competitively inhibited by the GLTFKSL peptide (Fig. 2B). GLTFKSL Abs recognized full-length recombinant PPP2R1A protein, whereas control IgGs were completely nonreactive (Fig. 2C).

Reciprocal immunoprecipitation experiments (Fig. 2D) and transmission EM (Fig. 2E and Fig. S2A–F) with a commercially available PPP2R1A Ab or the GLTFKSL Ab corroborated our results and revealed the presence of PPP2R1A on the membrane surface of C8161 melanoma cells. Interestingly, the PPP2R1A protein seems to be mainly located on membrane blebs that are potentially part of the leading edge of migrating melanoma cells (Fig. S2). To confirm additionally the identity of the PPP2R1A protein, we silenced PPP2R1A protein expression in C8161 melanoma cells with lentiviral shRNA constructs. Protein knockdown was confirmed by immunoblotting with either PPP2R1A or GLTFKSL Abs (Fig. 2F).

Next, to investigate whether PPP2R1A membrane expression is associated with melanoma metastasis, PPP2R1A cell surface expression was measured by FACS with a panel of 14 melanoma cell lines (Fig. 2G). Our analysis revealed a 40% increase in membrane expression of PPP2R1A in MeWo, UACC 62, C8161, and WM2664, which correlates with reported PPP2R1A microarray differential expression (23). More importantly, PPP2R1A overexpression correlated with metastatic potential in these cell lines from their original source (i.e., MeWo LN metastasis). Altogether, these results indicate that PPP2R1A is the antigen for the GLTFKSL Ab and further implicate its role in melanoma progression and metastasis.

**Lymphatic–Melanoma Cell Interaction Is Mediated by PPP2R1A.** Peptides recovered after the last round of LyV screening aligned with the primary sequence of PPP2R1A. Several peptides were found to mimic amino acid stretches in the PPP2R1A protein. Interestingly, the GLTFKSL peptide was also found to align near the C terminus of PPP2R1A (Fig. S3). The fact that GLTFKSL mimics a linear sequence found in native PPP2R1A protein suggests that we identified a linear epitope. When mapping protein–protein interactions with combinatorial peptide libraries, linear epitopes are adjacent residues in the primary protein sequence as opposed to conformational epitopes that comprise amino acids that are distant in the primary sequence but brought together in the native folded conformation. The combination of a putative linear epitope with (i) GLTFKSL phage binding to LECs and C8161 melanoma cells and (ii) Abs raised against GLTFKSL binding the PPP2R1A protein expressed on the cell surface indicated that PPP2R1A may form homodimers that can potentially mediate a heterotypic cell–cell interaction between the lymphatic endothelium–metastatic melanoma cell interface.

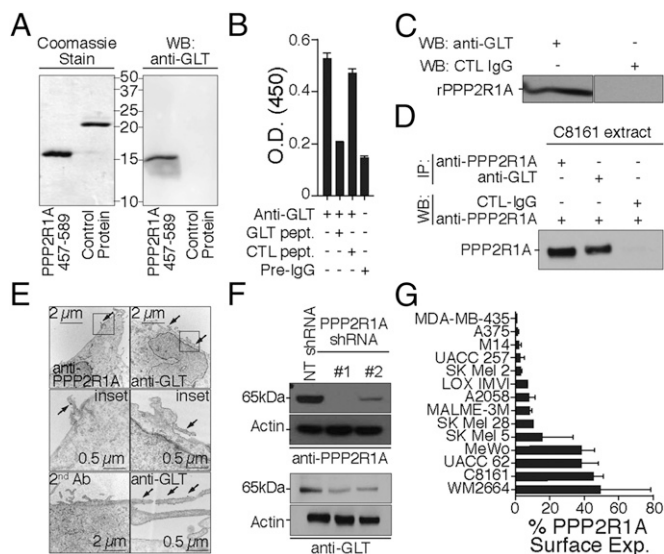


**Fig. 2.** GLTFKSL peptide is the molecular mimic of PPP2R1A. (A, Left) Expression of the truncated PPP2R1A 457–589 and a control protein from the microarray were verified by Coomassie blue staining. (A, Right) Anti-GLTFKSL Ab recognizes the truncated recombinant PPP2R1A protein by Western blot. (B) Binding specificity of GLTFKSL Ab to truncated recombinant PPP2R1A. The Ab reactivity against the recombinant protein was inhibited by addition of GLTFKSL peptide. (C) Anti-GLTFKSL recognizes recombinant human PPP2R1A by Western blot. (D) Reciprocal immunoprecipitation. Both anti-PPP2R1A and anti-GLTFKSL immunoprecipitate PPP2R1A from C8161 melanoma cell extracts. (E) Transmission EM of anti-GLTFKSL and anti-PPP2R1A binding to C8161 cells. Secondary Abs labeled with 18-nm gold particles were used for detection. (F) Silencing of PPP2R1A by shRNA in C8161 melanoma cells. Silencing was confirmed by immunoblotting with the anti-PPP2R1A and anti-GLTFKSL Abs. NT shRNA was used as control vector. (G) Cell surface binding of anti-PPP2R1A to a panel of human melanoma cell lines. The percentage of cell surface binding as analyzed by FACS is depicted as mean  $\pm$  SD. Rabbit IgG was used as a negative control. IP, immunoprecipitation; WB, Western blot.

To investigate whether a homophilic PPP2R1A–PPP2R1A interaction mediated by the GLT peptide sequence occurs, we first immobilized GLTFKSL or control peptides on 96-well plates in a modified ELISA binding assay. In this scenario, GLTFKSL phage should bind to GLTFKSL peptide. We observed specific binding of GLTFKSL phage to synthetic GLTFKSL peptide, whereas no binding was observed to control peptides (CTL1 and CTL2) or BSA (Fig. 3A). In addition, we immunocaptured native PPP2R1A from C8161 cell extracts with the commercially available PPP2R1A or the GLTFKSL Abs. GLTFKSL phage bound specifically to proteins immunoprecipitated by either the PPP2R1A Ab or the GLTFKSL Ab compared with a control Ab and insertless phage (Fig. 3B). Next, binding of the GLTFKSL peptide to C8161 melanoma with reduced PPP2R1A expression (PPP2R1A shRNA) was reduced by about 50% compared with nontargeted (NT) control (shRNA) cells (Fig. 3C) with the Bio-panning and Rapid Analysis of Selective Interactive Ligands methodology.

To examine further whether PPP2R1A mediates heterotypic cell–cell interaction, lymphatic cells (HDLECs) were plated and allowed to form a monolayer. Next, C8161 cells were labeled with carboxyfluorescein succinimidyl ester (Fig. S4), mixed with the highest nontoxic concentrations of anti-PPP2R1A or GLTFKSL peptide (previously determined), and incubated at normal growth conditions. Knockdown (PPP2R1A shRNA) and NT shRNA control cells were also prepared and evaluated. Melanoma cell adhesion was significantly impaired when anti-PPP2R1A Ab (10  $\mu$ g/mL) was added into the coculture (Fig. 3D) compared with

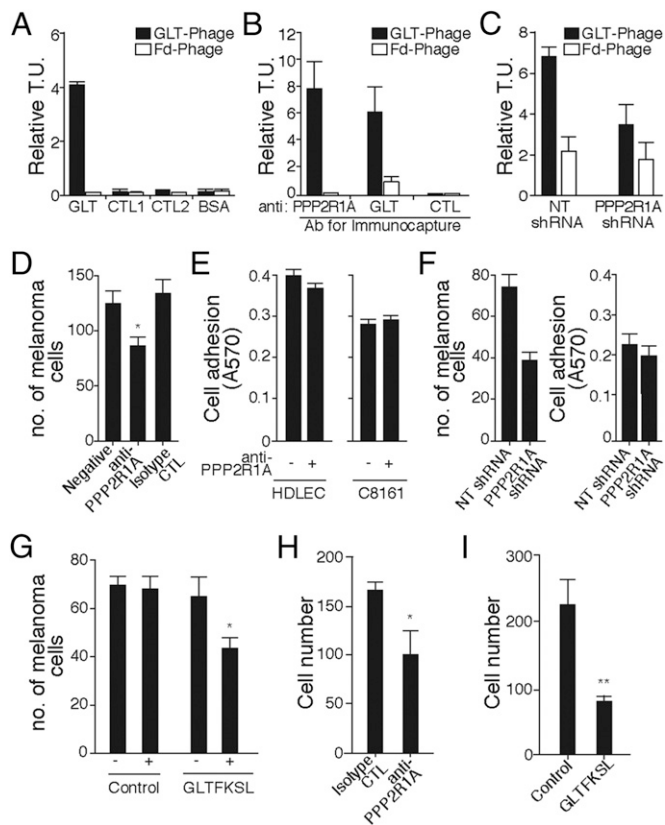


**Fig. 3.** PPP2R1A mediates the cell–cell interaction between LECs and melanoma. (A) GLTFKSL phage bound specifically to the GLTFKSL peptide compared with control peptides, BSA, and insertless phage. (B) PPP2R1A was immunocaptured from C8161 cell extracts with the anti-PPP2R1A and anti-GLTFKSL Abs. GLTFKSL phage bound to both immunocaptured proteins compared with control. All relative transducing units (T.U.) were expressed as means  $\pm$  SEMs. (C) The Biopanning and Rapid Analysis of Selective Interactive Ligands method was used to evaluate binding of GLTFKSL phage to C8161 cells stably transduced with PPP2R1A shRNA or NT shRNA. Binding of GLTFKSL phage to PPP2R1A-silenced cells was reduced by about 50%. Insertless control phage (Fd phage) served as a negative control. (D) Ab against PPP2R1A inhibits cell–cell interaction between melanoma and lymphatic cells. (E) Lymphatic and melanoma cell adhesion to the ECM was evaluated in vitro with or without addition of anti-PPP2R1A Ab. (F, Left) Silencing of PPP2R1A in C8161 decreases melanoma cell attachment to LECs. (F, Right) Cell adhesion to the ECM was not compromised after PPP2R1A knockdown. (G) Melanoma–lymphatic cell interaction inhibited by the GLTFKSL peptide. Cell migration is mediated by surface expression of PPP2R1A. (H) Anti-PPP2R1A Ab. (I) GLTFKSL peptide. CTL, control. \* $P < 0.05$ ; \*\* $P < 0.01$ .

the isotype control. Cell toxicity or difference in cell adhesion of both HDLECs and C8161 to the substrate (Fig. 3E) was not observed after addition of anti-PPP2R1A. However, similar inhibition of melanoma cell attachment was observed in PPP2R1A-silenced C8161 cells (Fig. 3F) or cells treated with the GLTFKSL peptide (Fig. 3G). PPP2R1A knockdown C8161 cells showed a significant, approximately twofold reduction in the number of melanoma cells cultured on a monolayer of HDLECs compared with C8161 cells transduced with control NT shRNA. No significant changes in cell proliferation or cell adhesion to the HDLEC monolayer substrate were observed when C8161 was stably transduced with PPP2R1A shRNA (Fig. 3F, Right). Addition of GLTFKSL peptide (Fig. 3G) decreased melanoma cell attachment to lymphatic cells by 20% relative to control peptide or in the absence of peptide treatment. Interestingly, melanoma cell migration was significantly inhibited in the presence of the anti-PPP2R1A Ab (10  $\mu$ g/mL) or the GLTFKSL peptide (10  $\mu$ M). Anti-PPP2R1A Ab significantly

reduced C8161 cell migration by 1.6-fold compared with untreated cells (Fig. 3H). This effect was more robust when melanoma cells were incubated with the GLTFKSL peptide (Fig. 3I), reducing cell migration by 2.8-fold. Overall, these data show that PPP2R1A mediates a heterotypic cell–cell interaction through homodimer formation.

**PPP2R1A Is Accessible in Vivo.** Next, localization of the PPP2R1A protein was assessed in orthotopic C8161 tumor xenografts by immunofluorescence. Frozen sections of explanted tumors were coimmunostained with Abs against PPP2R1A, CD34 (a vascular endothelial protein), and the LyV protein podoplanin. PPP2R1A was ubiquitously expressed within tumor cells. Moreover, PPP2R1A extensively colocalized with LECs, whereas colocalization was not observed in blood vessels (Fig. 4A). To determine whether PPP2R1A was accessible on melanoma and LECs in vivo, we evaluated the biodistribution of GLTFKSL phage in C8161 tumors in tumor-bearing mice by immunohistochemistry with antiphage Abs. We show that the targeted GLTFKSL phage selectively and specifically bound to melanoma tumors compared with a control phage and control organs (Fig. 4B). High levels of PPP2R1A expression were also found on C8161 tumor cells relative to controls, thus confirming that PPP2R1A is an accessible tumor target in vivo (Fig. 4C).

**PPP2R1A Expression on Melanoma Patient Biopsy Samples Correlates with Poor Outcome.** Thirty-one human patient samples with metastatic melanoma (grade IV) were evaluated to examine the clinical relevance of PPP2R1A expression on LECs and melanoma cells. Melanoma cells as well as LECs were isolated and subjected to FACS analysis to evaluate cell surface expression. All 31 patient samples had high (>50%) PPP2R1A cell surface expression for both cell types. More importantly, a statistically significant correlation of PPP2R1A expression between melanoma and LECs was found (Pearson correlation;  $P = 0.017$ ) (Fig. 5A). PPP2R1A expression on patient-derived LECs was ranked from high to low and correlated with the matched melanoma cell sample from the same patient. A critical issue in protein discovery with combinatorial screenings is to test the putative marker on subjects that were not included in the original assay design. Histological analysis of human melanoma samples at different stages showed high expression of PPP2R1A in primary tumor samples, in-transit metastasis, and LN metastasis (Fig. 5B).

Our data show that the two-arm approach developed in this report allows identification of singular and relevant cell surface receptors. Furthermore, we established that PPP2R1A, a previously unrecognized cell surface receptor, contributes to cell–cell interactions between melanoma and lymphatic cells. Finally, increased expression of PPP2R1A in both lymphatic and tumor cells during melanoma progression indicates that PPP2R1A may play an important role during melanoma invasion and metastasis through the lymphatic vasculature. Additional studies will elucidate and accelerate understanding of cell–cell interactions within the context of LyV biology and melanoma metastasis.

## Discussion

In this report, we show that tailoring combinatorial library selection of phage display to use available patient samples ex vivo in parallel with traditional in vitro experiments can be successfully used to identify potentially clinically relevant tumor biomarkers. The successful isolation and validation of PPP2R1A as a candidate biomarker of melanoma metastasis through interactions between melanoma tumor cells and LECs indicate the potential of this approach. PPP2R1A is the scaffolding subunit A of the protein phosphatase 2A (PP2A), one of four major serine/threonine protein phosphatases. PP2A plays an important role in cell proliferation, death, mobility, cell cycle control, and development and is involved in the regulation of numerous signaling

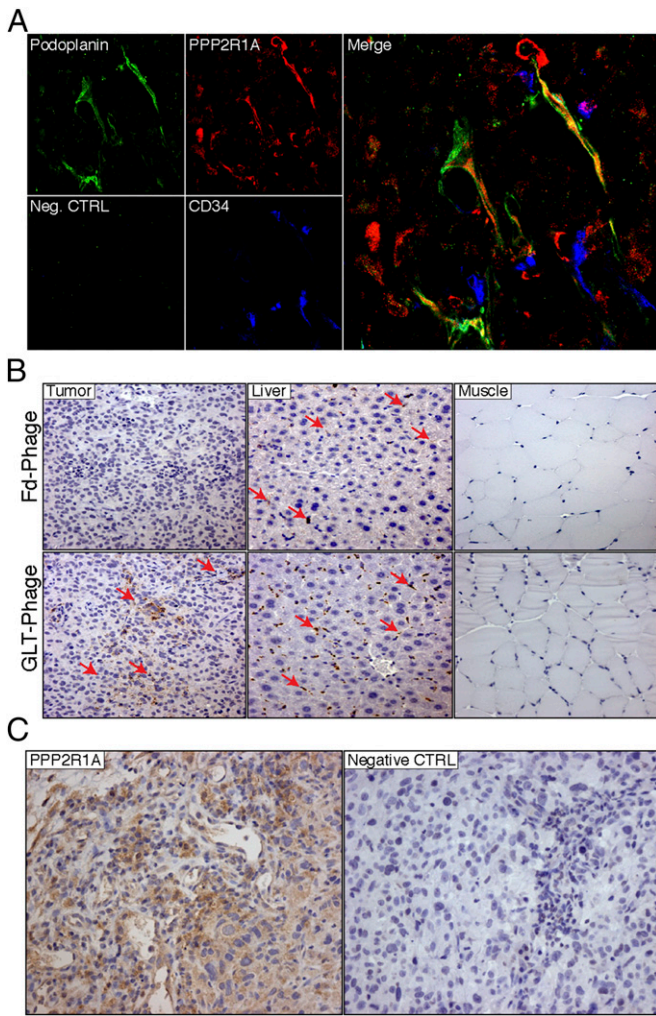


**Fig. 4.** PPP2R1A is expressed on LyVs in vivo. (A) Confocal microscopy was performed on C8161 tumor frozen sections stained with PPP2R1A (red), Podoplanin (green), and CD34 (blue). Colocalization (yellow) of PPP2R1A and Podoplanin is depicted in the merged image. Neg. CTRL, negative control. (B) Immunohistochemical analysis of GLTFKSL phage homing. Positive staining (red arrows) is shown in the tumor of GLTFKSL-injected mice, whereas insertless phage staining in the tumor is negative. Muscle was the negative control organ. Liver is part of the reticuloendothelial system, and therefore, phage is present. Representative pictures are shown (magnification: 200 $\times$ ). (C) PPP2R1A expression in C8161 tumors. PPP2R1A is highly expressed in C8161 tumors as shown by immunohistochemistry. CTRL, control. (Magnification: 200 $\times$ .)

pathways (24, 25). PP2A exists in two general forms—a heterodimeric core enzyme and a heterotrimeric holoenzyme. The core enzyme consists of the scaffolding subunit A and a catalytic subunit C, and each can exist as two isoforms. The PP2A core enzyme interacts with a large number of alternative forms of the variable regulatory subunit B to assemble into a holoenzyme, which recognizes many different substrates (24, 25). Alterations affecting different subunits or isoforms have detrimental effects on phosphatase function and have been shown to promote tumorigenesis (26, 27). Several mutations of the PPP2R1A isoform have been reported in breast and lung cancers; ovarian, uterine, and endometrial carcinomas; and malignant melanoma (22, 27–30). Because loss of PPP2R1A in mice is lethal, at least a minimal amount of PPP2R1A is required to maintain cell viability (31, 32). Considering the myriad functions that can be affected by alterations of the PPP2R1A isoform, it is difficult to designate its role

in tumorigenesis, and efforts to reconcile the diverse functions of PPP2R1A are ongoing (26, 27, 33).

To the best of our knowledge, there are no reports of cell surface expression of PPP2R1A, its expression in the extracellular environment, or its function other than its activity as a phosphatase enzyme complex. Our data indicate that extracellular PPP2R1A mediates interactions between LECs and melanoma cells. Thus, an extracellular function for PPP2R1A in melanoma through cell–cell interactions with the LECs, as revealed here, could be relevant for a number of different cancers and is possibly independent of the PP2A enzyme. The role of scaffold proteins in cell adhesion and their recruitment based on chemical or biophysical signals are well-described, and the implications of this knowledge in tumor invasiveness, aggressiveness, and metastasis formation have been shown (34, 35). Our findings are consistent with this knowledge and were anticipated with an unbiased combinatorial peptide library in the phage panning and selection scheme as described above. Proteins are selected based on their expression profile on the cell surface and their availability or accessibility to circulating ligands (36). This approach for identifying and validating ligand–receptor interactions has previously shown a novel extracellular function for the CRKL protein in tumorigenesis (37). The tumor microenvironment may induce this heretofore unrecognized, to our knowledge,

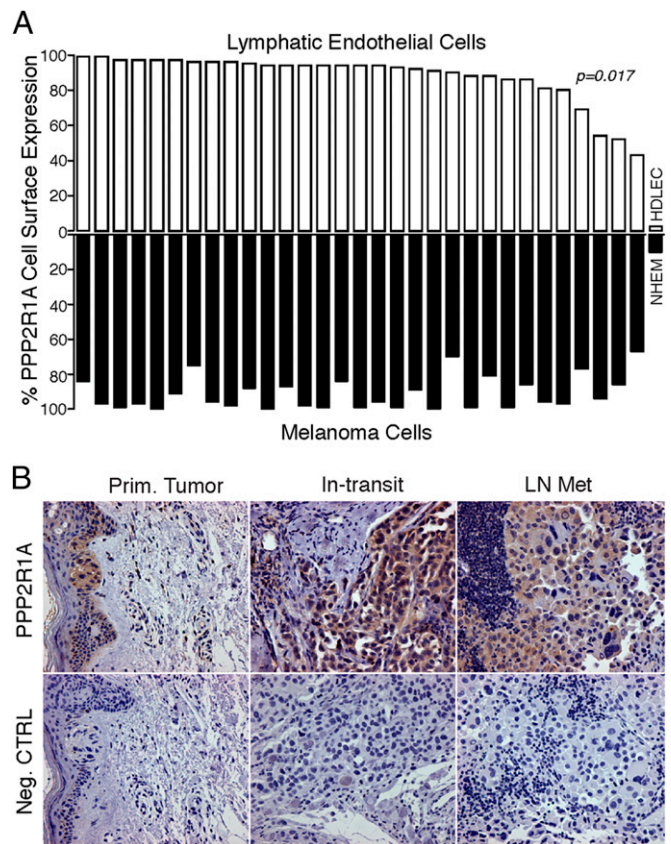


**Fig. 5.** PPP2R1A expression on melanoma patient samples. (A) PPP2R1A is expressed on the cell surface of human metastatic melanoma samples (grade IV). Flow cytometry analysis of melanoma samples is graphically represented as a waterfall blot. A positive correlation is observed between expression of PPP2R1A on the surface of LECs and melanoma cells as calculated by the Pearson correlation method ( $r = 4$ ,  $P = 0.017$ ). NHEM, normal human melanocyte. (B) Histological analysis of human melanoma samples. Primary melanoma (Prim. Tumor), in-transit metastasis (In-transit), and LN metastasis (LN Met) samples stain positive for PPP2R1A. Neg. CTRL, negative control. (Magnification: 200 $\times$ .)

functionality, and these results show the biological significance of these extracellular roles in tumor cell proliferation and migration.

Homodimer formation described here is reminiscent of another report, where a homophilic interaction of the cell surface glycoprotein MUC18 was observed between melanoma cells and B-1 lymphocytes (38). It was suggested that the surface expression of MUC18 may be differentially regulated on the two separate cell surfaces and that the interaction of the two cell types through a homophilic MUC18–MUC18 ligand–receptor system influences melanoma metastasis (38). The fact that both the MUC18 and PPP2R1A homodimeric protein complexes involve scaffold proteins is unsurprising and indicative of the translational potential for evaluating scaffold proteins and their cell–cell junctions for markers of tumor progression and metastasis. Indeed, additional experiments are needed to understand the functional role of PPP2R1A on the cell surfaces of the LECs and melanoma cells and the regulatory mechanism that influences its extracellular expression.

- Jain RK (2003) Molecular regulation of vessel maturation. *Nat Med* 9(6):685–693.
- Pepper MS, Skobe M (2003) Lymphatic endothelium: Morphological, molecular and functional properties. *J Cell Biol* 163(2):209–213.
- Mandriota SJ, et al. (2001) Vascular endothelial growth factor-C-mediated lymphangiogenesis promotes tumour metastasis. *EMBO J* 20(4):672–682.
- Stacker SA, et al. (2001) VEGF-D promotes the metastatic spread of tumor cells via the lymphatics. *Nat Med* 7(2):186–191.
- Alitalo A, Detmar M (2012) Interaction of tumor cells and lymphatic vessels in cancer progression. *Oncogene* 31(42):4499–4508.
- Balch CM, et al. (2009) Final version of 2009 AJCC melanoma staging and classification. *J Clin Oncol* 27(36):6199–6206.
- Gershenwald JE, Bar-Eli M (2004) Gene expression profiling of human cutaneous melanoma: Are we there yet? *Cancer Biol Ther* 3(1):121–123.
- Luca MR, Bar-Eli M (1998) Molecular changes in human melanoma metastasis. *Histol Histopathol* 13(4):1225–1231.
- Zigler M, Dobroff AS, Bar-Eli M (2010) Cell adhesion: Implication in tumor progression. *Minerva Med* 101(3):149–162.
- Hirakawa MI, Iritani BM, Ruddell A (2007) Tumor-induced sentinel lymph node lymphangiogenesis and increased lymph flow precede melanoma metastasis. *Am J Pathol* 170(2):774–786.
- Hirakawa S, et al. (2007) VEGF-C-induced lymphangiogenesis in sentinel lymph nodes promotes tumor metastasis to distant sites. *Blood* 109(3):1010–1017.
- Hirakawa S, et al. (2005) VEGF-A induces tumor and sentinel lymph node lymphangiogenesis and promotes lymphatic metastasis. *J Exp Med* 201(7):1089–1099.
- Qian CN, et al. (2006) Preparing the “soil”: The primary tumor induces vasculature reorganization in the sentinel lymph node before the arrival of metastatic cancer cells. *Cancer Res* 66(21):10365–10376.
- Deramchia K, et al. (2012) In vivo phage display to identify new human antibody fragments homing to atherosclerotic endothelial and subendothelial tissues [corrected]. *Am J Pathol* 180(6):2576–2589.
- Cao L, et al. (2012) Phage-based molecular probes that discriminate force-induced structural states of fibronectin in vivo. *Proc Natl Acad Sci USA* 109(19):7251–7256.
- Cardó-Vila M, et al. (2010) From combinatorial peptide selection to drug prototype (II): Targeting the epidermal growth factor receptor pathway. *Proc Natl Acad Sci USA* 107(11):5118–5123.
- Rangel R, et al. (2012) Combinatorial targeting and discovery of ligand-receptors in organelles of mammalian cells. *Nat Commun* 3:788.
- Gershenwald JE, Ross MI (2011) Sentinel-lymph-node biopsy for cutaneous melanoma. *N Engl J Med* 364(18):1738–1745.
- Mu H, et al. (2012) Lysophosphatidic acid induces lymphangiogenesis and IL-8 production in vitro in human lymphatic endothelial cells. *Am J Pathol* 180(5):2170–2181.
- Hemmings BA, et al. (1990) alpha- and beta-forms of the 65-kDa subunit of protein phosphatase 2A have a similar 39 amino acid repeating structure. *Biochemistry* 29(13):3166–3173.
- Giordano RJ, Cardó-Vila M, Lahdenranta J, Pasqualini R, Arap W (2001) Biopanning and rapid analysis of selective interactive ligands. *Nat Med* 7(11):1249–1253.
- Jones S, et al. (2010) Frequent mutations of chromatin remodeling gene ARID1A in ovarian clear cell carcinoma. *Science* 330(6001):228–231.
- Su DM, et al. (2009) Two types of human malignant melanoma cell lines revealed by expression patterns of mitochondrial and survival-apoptosis genes: Implications for malignant melanoma therapy. *Mol Cancer Ther* 8(5):1292–1304.
- Janssens V, Goris J (2001) Protein phosphatase 2A: A highly regulated family of serine/threonine phosphatases implicated in cell growth and signalling. *Biochem J* 353(Pt 3):417–439.
- Shi Y (2009) Serine/threonine phosphatases: Mechanism through structure. *Cell* 139(3):468–484.
- Eichhorn PJ, Creighton MP, Bernards R (2009) Protein phosphatase 2A regulatory subunits and cancer. *Biochim Biophys Acta* 1795(1):1–15.
- Mumby M (2007) PP2A: Unveiling a reluctant tumor suppressor. *Cell* 130(1):21–24.
- Calin GA, et al. (2000) Low frequency of alterations of the alpha (PPP2R1A) and beta (PPP2R1B) isoforms of the subunit A of the serine-threonine phosphatase 2A in human neoplasms. *Oncogene* 19(9):1191–1195.
- McConechy MK, et al.; Australian Ovarian Cancer Study Group (2011) Subtype-specific mutation of PPP2R1A in endometrial and ovarian carcinomas. *J Pathol* 223(5):567–573.
- Kuhn E, et al. (2012) Identification of molecular pathway aberrations in uterine serous carcinoma by genome-wide analyses. *J Natl Cancer Inst* 104(19):1503–1513.
- Chen W, Arroyo JD, Timmons JC, Possemato R, Hahn WC (2005) Cancer-associated PP2A Aalpha subunits induce functional haploinsufficiency and tumorigenicity. *Cancer Res* 65(18):8183–8192.
- Ruediger R, Ruiz J, Walter G (2011) Human cancer-associated mutations in the Aα subunit of protein phosphatase 2A increase lung cancer incidence in Aα knock-in and knockout mice. *Mol Cell Biol* 31(18):3832–3844.
- Wei D, et al. (2013) Inhibition of protein phosphatase 2A radiosensitizes pancreatic cancers by modulating CDC25C/CDK1 and homologous recombination repair. *Clin Cancer Res* 19(16):4422–4432.
- Berrier AL, Yamada KM (2007) Cell-matrix adhesion. *J Cell Physiol* 213(3):565–573.
- Miles FL, Sikes RA (2014) Insidious changes in stromal matrix fuel cancer progression. *Mol Cancer Res* 12(3):297–312.
- Ozawa MG, et al. (2008) Beyond receptor expression levels: The relevance of target accessibility in ligand-directed pharmacodelivery systems. *Trends Cardiovasc Med* 18(4):126–132.
- Mintz PJ, et al. (2009) An unrecognized extracellular function for an intracellular adapter protein released from the cytoplasm into the tumor microenvironment. *Proc Natl Acad Sci USA* 106(7):2182–2187.
- Staquicini FI, et al. (2008) A subset of host B lymphocytes controls melanoma metastasis through a melanoma cell adhesion molecule/MUC18-dependent interaction: Evidence from mice and humans. *Cancer Res* 68(20):8419–8428.

## Materials and Methods

**Patient Samples.** This study adheres strictly to current medical ethics recommendations and guidelines regarding human research, and it has been reviewed and approved by the Clinical Ethics Service, the Institutional Biohazard Committee, the Clinical Research Committee, and the Institutional Review Board of The University of Texas MD Anderson Cancer Center.

**Animals.** Six- to eight-week-old nude mice were purchased from Charles River or The Jackson Laboratories. All animal work followed standard procedures approved by The University of Texas MD Anderson Cancer Center.

**Statistics.** A correlation test was performed with R (The R Project for Statistical Computing) according to the Pearson correlation method. SEM and SD were calculated with the GraphPad Prism program.

Additional methods are described in [SI Materials and Methods](#).

**ACKNOWLEDGMENTS.** This work was supported by awards from the Gillson Longenbaugh Foundation and the American Recovery and Reinvestment Act of 2009, a Cancer Center Support grant (to University of New Mexico Cancer Center), and a Department of Defense grant (to W.A. and R.P.)